Chemical Papers
https://doi.org/10.1007/s11696-020-01188-0

ORIGINAL PAPER

Synthesis and biological evaluation of innovative thiourea derivatives as PHGDH inhibitors

Jiawei Xiang[1] · Lei Tao[2] · Yue Zhou[1,2] · Yuping Tan[1,2] · Zicheng Li[1] · Yinglan Zhao[1] · Qingxiang Sun[2] · Youfu Luo[2]

Received: 22 October 2019 / Accepted: 7 May 2020

Abstract

In order to discover novel compounds with inhibitory activity against 3-phosphoglycerate dehydrogenase (PHGDH), a series of thiourea derivatives were designed and synthesized based on the structural modification of compound **5d**. Compound **5d** emerged from the visual database of ChemDiv of 200,000 small molecules by docking score ranking. Inhibition experiments on PHGDH activity of newly synthesized compounds were performed in vitro. Compounds with more than 30% inhibitory rate at 25 μM on PHGDH were screened for IC_{50} measurement. Anti-proliferative activity of **4a**, **5a**, **6e**, **6n** against A2780, MDA-MB-468, MDA-MB-231 and HEK293T in vitro was evaluated. The results showed that the compound **4a** displayed the best inhibitory activity on PHGDH among the newly synthesized compounds, and the compounds **4a**, **5a**, **6n** had a better proliferation inhibition effect on human A2780 cell line than **NCT-503** reported previously. In addition, 2D interaction diagrams revealed potential action modes of active compounds with PHGDH.

Keywords 3-Phosphoglycerate dehydrogenase (PHGDH) · Thiourea derivatives · Virtual screening · Proliferation inhibition effect · 2D interaction diagrams

Introduction

The phosphoglycerate dehydrogenase (PHGDH) is the first and important branching enzyme in the glycolytic-serine biosynthetic pathway (Pacold et al. 2016; Ravez et al. 2017; Reid et al. 2018). PHGDH oxidizes glycolysis intermediate 3-phosphoglycerate (3-PG) to 3-phosphohydroxypyruvate (p-Pyr), and finally serine is synthesized through a series of enzymes (Sullivan et al. 2019; Truong et al. 2017; Weinstabl et al. 2019). Serine plays an important role in the synthesis of proteins and other biomolecules required for cell proliferation, such as nucleotides, phosphatidylserine and sphingosine (Ducker et al. 2017). Recent studies have found that PHGDH is highly expressed in a range of tumors. It is also related to tumor cell growth and low survival rate of tumor patients (Jia et al. 2016; Jing et al. 2015; Mattaini et al. 2015).

In previous studies, PHGDH has been confirmed as a promising target in cancer by target validation, performed in vitro and in vivo knockdown models (Gromova et al. 2015; Ou et al. 2015; Vandekeere et al. 2018). So far, there have been few reports of PHGDH small molecule inhibitors. There were only three major PHGDH inhibitors published in peer-reviewed, namely **CBR-5884** ($IC_{50} = 33 \pm 12$ μM), **NCT-503** ($IC_{50} = 2.5 \pm 0.6$ μM) and **PKUMDL-WQ-2101** ($IC_{50} = 34.8 \pm 3.6$ μM) (Pacold et al. 2016; Wang et al. 2017). CBR-5884 and NCT-503 were obtained by high-throughput screening (HTS), and the third type was PHGDH allosteric inhibitor discovered by virtual screening (Mullarky et al. 2019; Reid et al. 2018). These three inhibitors had similar potency in vitro biochemical assays. They had moderate selectivity for PHGDH and inhibited PHGDH activity in a noncompetitive manner (Ravez et al. 2017; Wang et al. 2017).

In order to further search for PHGDH small molecule inhibitors with other novel structures, a virtual screening was conducted by Schrodinger_Suites_2018-1, a virtual docking

Electronic supplementary material The online version of this article (https://doi.org/10.1007/s11696-020-01188-0) contains supplementary material, which is available to authorized users.

✉ Zicheng Li
sculzc@scu.edu.cn

[1] School of Chemical Engineering, Sichuan University, Chengdu 610065, Sichuan, People's Republic of China

[2] State Key Laboratory of Biotherapy and Cancer Center, West China Hospital, West China Medical School, Chengdu 610041, Sichuan, People's Republic of China

Published online: 24 May 2020

software. Compound **5d** emerged from the visual database of ChemDiv of 200,000 small molecules. The molecular docking procedure was performed by using glide docking program of Schrodinger_Suites_2018-1. The 200,000 small molecule databases were used to dock using standard precision. We ranked the docking scores of all molecules. **NCT-503** was used as the control. The number of compounds with docking score above 8.0 was about 65 (**NCT-503** was 9.124). We considered synthesis difficulty and availability of raw materials and then selected two molecules **116** and **5d** (docking scores were 8.806 and 8.987, respectively)(Fig. 1). Partial reason for selecting compound **5d** was structural similarity with **NCT-503**. This increased our confidence that compound 5d had great activity. The two molecules were then synthesized, and their inhibitory activity on PHGDH was measured (**116**, IC_{50} = 174 μM; **5d**, IC_{50} = 56 μM). Due to the better activity against PHGDH, Compound **5d** was selected as a lead compound.

Due to the structural similarity, the piperazine structure of **NCT-503** and the SAR of piperazine-1-thiourea compounds were referred (Pacold et al. 2016; Rohde et al. 2018). We synthesized a series of **5d** derivatives and discussed structure–activity relationships of newly synthesized molecules.

Firstly, to explore the effect of different piperidine or piperazine structures on the activity of compound **5d**, we modified the piperidine structure of **5d** to obtain compounds **4b**, **5e**, **5f** and **6o**. The inhibition rates of compounds **4b**, **5d**, **5e**, **5f** and **6o** at 25 μM were 20%, 30%, 23%, 24% and 31%, respectively. We found that not only **6o** maximized the activity of **5d** maximally, but the piperazine structure of **6o** was also more easily synthesized than the piperidine structure of **5d**. So, compound **6o** was selected as the starting point for our next optimization. Then, we maintained the piperazine structure of compound **6o** and changed the aromatic structure on the other side of the thiocarbonyl group. We used different substituted benzene rings, aromatic heterocyclic rings and cycloalkyl groups as R groups to explore the effect of them on the activity of the compounds. A series of compounds **6a**–**n** were obtained. The results showed that aromatic heterocyclic rings had better activity than other groups, and 3-(oxazol-5-yl) phenyl was the best active of all R groups. Compound **6n** showed the best inhibition rate of 47% at 25 μM. Finally, compound **6n** was replaced with different piperazine or piperidine structures again to obtain compounds **4a**, **5a**–**c**.

Moreover, anti-proliferative activity of **4a**, **5a**, **6e** and **6n** against A2780, MDA-MB-468, MDA-MB-231 and HEK293T in vitro was evaluated. To understand the potential action modes of molecules and protein, 2D interaction diagrams were generated by Schrodinger_Suites_2018-1.

Experimental

Chemistry

Materials and instruments

All the reagents were purchased from commercial suppliers without further purification unless otherwise specified. Melting points were determined with a capillary method and are uncorrected. IR spectra were recorded on a Spectrum Two Li10014 spectrometer. ^{1}H NMR and ^{13}C NMR spectra were recorded on a Bruker Avance 400 MHz spectrometer. NMR spectra were recorded in DMSO-d_6 or $CDCl_3$ solutions at room temperature (20 ± 2 °C). ^{1}H and ^{13}C chemical shifts were quoted in parts per million downfield from TMS. ESI–MS spectra were recorded on a Bruker Esquire 3000 instrument. High-resolution mass spectra (HRMS) were obtained on a MicrOTOF-Q II mass spectrometer with an ESI source (Waters, Manchester). Compound **NCT-503** was purchased from MCE. Other newly synthesized compounds were characterized by IR, ^{1}H NMR, ^{13}C NMR spectra and mass spectra.

Synthesis of compound 116

Compound **116** was prepared according to literature methods [Supporting Information] (Won et al. 2003).

General procedure for the preparation of intermediates 2

Add compound **1** (1 mmol) to a solution of di(1H-imidzazol-1-yl)methanethione (196 mg, 1.1 mmol) in 5 ml THF. The

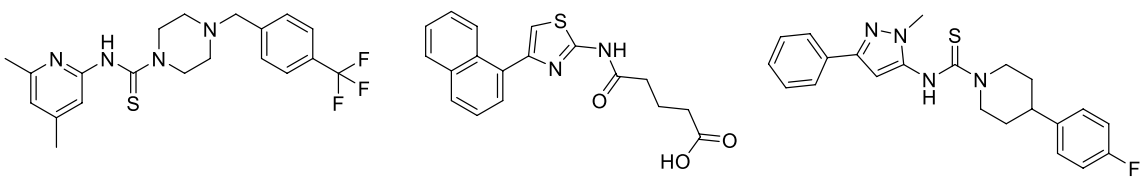

Fig. 1 Structures of PHGDH inhibitors **NCT-503**, **116** and **5d**

resulting reaction mixture was heated at 45 °C for 0.5–1.5 h. The reaction was then cooled to room temperature to give a mixture containing intermediate **2**.

The specific mass of compound **1** required for the reaction was: 3-chloro-4-fluoroaniline (146 mg, 1 mmol), thiazol-2-amine (100 mg, 1 mmol), 4-chloroaniline (128 mg, 1 mmol), 4-fluoroaniline (111 mg, 1 mmol), 1,3-dimethyl-1*H*-pyrazol-5-amine (111 mg, 1 mmol), 3-chloroaniline (128 mg, 1 mmol), 3,4-dichloroaniline (162 mg, 1 mmol), 4,4-dimethylcyclohexan-1-amine (127 mg, 1 mmol), 4-bromoaniline (172 mg, 1 mmol), naphthalen-1-amine (143 mg, 1 mmol), 4-(trifluoromethyl)aniline (161 mg, 1 mmol), [1,1′-biphenyl]-4-amine (169 mg, 1 mmol), 4-isopropylaniline (135 mg, 1 mmol), 3-(oxazol-5-yl)aniline (160 mg, 1 mmol), 1-methyl-3-phenyl-1*H*-pyrazol-5-amine (173 mg, 1 mmol).

Synthesis of compound 3

Piperazine (27.61 g, 320 mmol) was dissolved in THF (300 ml) by heating. 1-(Bromomethyl)-4-(trifluoromethyl) benzene (9.56 g, 40 mmol) was added dropwise to a solution of piperazine in THF under reflux. After being stirred overnight under reflux, the reaction mixture was cooled to room temperature, and the THF was removed by evaporation. The resulting residue was washed with aq. K_2CO_3, extracted with ethyl acetate, washed with sat. NaCl, dried with Na_2SO_4 and evaporated to dryness under vacuum to yield **3** (O'Dowd et al. 2017).

1-(4-(trifluoromethyl)benzyl)piperazine (3) Colorless liquid, yield: 86%; ^{1}H NMR (400 MHz, DMSO): δ 7.67 (d, J = 8.0 Hz, 2H), 7.52 (d, J = 8.0 Hz, 2H), 3.51 (s, 2H), 2.76–2.62 (m, 4H), 2.29 (s, 4H);^{13}C NMR (100 MHz, DMSO): δ 143.92, 129.84, 127.99 (q, J = 31.6 Hz), 125.43 (q, J = 3.8 Hz), 124.85 (q, J = 271.8 Hz), 62.58, 54.58, 46.07. HRMS Calcd. for $C_{12}H_{15}F_3N_2$ $[M+H]^+$ 245.1260, found 245.1259.

General procedure for the preparation of compounds 4, 5, 6

The mixture containing intermediate **2** was transferred to another vial containing a solution comprised of piperazine or piperidine derivatives (1 mmol), THF (3 ml), and triethylamine (0.14 ml, 1 mmol). An additional aliquot of THF (2 ml) was used to complete the transfer. The resulting reaction mixture was heated with stirring at 75 °C for 1.5–2.5 h. Then, the reaction mixture was concentrated and diluted with water and DCM. The layers were separated and the aqueous layer was reextracted with DCM. The combined organic layers were dried with Na_2SO_4 and concentrated in vacuo. After that, the resulting residue was purified via phase column chromatography (ethyl acetate/petroleum ether = 1:5–1:15) to give product **4**, **5** or **6**, respectively.

The specific mass of piperazine or piperidine derivatives required for the reaction was: 1-(4-(trifluoromethyl)benzyl) piperazine (244 mg, 1 mmol), 4-(4-fluorophenyl)piperidine (179 mg, 1 mmol), 1-(3-(trifluoromethyl)phenyl)piperazine (230 mg, 1 mmol), methyl 2-(piperidin-4-yl)acetate (157 mg, 1 mmol), 4-(3-chlorophenyl)piperidine (196 mg, 1 mmol).

***N*-(3-(oxazol-5-yl)phenyl)-4-(3-(trifluoromethyl)phenyl)piperazine-1-carbothio-amide (4a)** Yellow solid, yield: 65%; mp: 124.9–125.1 °C; IR (KBr, cm^{-1}): 3283, 3101, 2922, 2839, 1615, 1540, 1497, 1449, 1321, 787, 714, 691; ^{1}H NMR (400 MHz, DMSO-d_6): δ 9.53 (s, 1H), 8.44 (s, 1H), 7.70 (s, 1H), 7.67 (s, 1H), 7.51–7.38 (m, 3H), 7.36 (s, 1H), 7.21 (s, 2H), 7.09 (d, J = 7.6 Hz, 1H), 4.16–4.02 (m, 4H), 3.48–3.35 (m, 4H); ^{13}C NMR (100 MHz, DMSO-d_6): δ 181.88, 152.29, 151.08, 150.82, 142.22, 130.50, 130.43 (q, J = 31.0 Hz), 129.32, 127.74, 126.03, 124.92 (q, J = 272.5 Hz), 122.46, 121.35, 120.60, 118.95, 115.10 (q, J = 4.0 Hz), 111.25 (q, J = 4.0 Hz), 47.96, 47.42. HRMS Calcd. for $C_{21}H_{19}F_3N_4OS$ $[M+H]^+$ 433.1305, found 433.1311.

***N*-(1-methyl-3-phenyl-1*H*-pyrazol-5-yl)-4-(3-(trifluoromethyl) phenyl)piperazine-1-carbothioamide (4b)** White solid, yield: 60%; mp: 176.4–177.5 ℃; IR (KBr, cm^{-1}): 3122, 2931, 1610, 1509, 1476, 1443, 1363, 1307, 833, 767, 721, 697; ^{1}H NMR (400 MHz, $CDCl_3$): δ 7.77–7.69 (m, 2H), 7.37 (s, 1H), 7.36–7.32 (m, 3H), 7.30–7.23 (m, 1H), 7.12 (d, J = 7.8 Hz, 1H), 6.99 (s, 1H), 6.93 (d, J = 8.4 Hz, 1H), 6.37 (s, 1H), 3.99–3.88 (m, 4H), 3.69 (s, 3H), 3.27–3.16 (m, 4H); ^{13}C NMR (100 MHz, DMSO-d_6): δ 181.98, 151.03, 148.25, 140.34, 134.04, 130.51, 130.44 (q, J = 31.1 Hz) 129.06, 127.76, 125.10, 124.92 (q, J = 272.6 Hz), 118.97, 115.16 (q, J = 4.0 Hz), 111.27 (q, J = 3.6 Hz), 100.39, 48.06, 47.33, 36.14. HRMS Calcd. for $C_{22}H_{22}F_3N_5S$ $[M+H]^+$ 446.1621, found 446.1619.

4-(4-fluorophenyl)-*N*-(3-(oxazol-5-yl)phenyl)piperidine-1-carbothioamide (5a) Yellow solid, yield: 65%; mp: 78.3–79.7 ℃; IR (KBr, cm^{-1}): 2923, 2853, 1618, 1532, 1508, 1439, 1323, 832, 790, 770, 714, 688; ^{1}H NMR (400 MHz, DMSO-d_6): δ 9.41 (s, 1H), 8.45 (s, 1H), 7.73–7.61 (m, 2H), 7.47 (d, J = 7.8 Hz, 1H), 7.40 (t, J = 7.8 Hz, 1H), 7.37–7.27 (m, 3H), 7.13 (t, J = 9.0 Hz, 2H), 4.92 (d, J = 13.2 Hz, 2H), 3.15 (t, J = 12.0 Hz, 2H), 2.90 (dd, J = 16.4, 8.0 Hz, 1H), 1.91–1.80 (m, 2H), 1.65 (qd, J = 12.8, 3.8 Hz, 2H); ^{13}C NMR (100 MHz, DMSO-d_6): δ 181.41, 161.25 (d, J = 241.8 Hz), 152.27, 150.87, 142.49, 142.00 (d, J = 2.9 Hz), 129.26, 129.00 (d, J = 7.9 Hz), 127.67, 125.83,

122.41, 121.08, 120.33, 115.55 (d, $J = 20.9$ Hz), 49.20, 41.34, 33.36. HRMS Calcd. for $C_{21}H_{20}FN_3OS$ $[M + H]^+$ 382.1384, found 382.1389.

4-(3-Chlorophenyl)-*N*-(3-(oxazol-5-yl)phenyl)piperidine-1-carbothioamide (5b) Light green solid, yield: 60%; mp: 146.2–147.8 ℃; IR (KBr, cm^{-1}): 3233, 3088, 2933, 2851, 1618, 1594, 1576, 1535, 1503, 1473, 1442, 1407, 1322, 900, 825, 797, 733, 692; ^{1}H NMR (400 MHz, DMSO-d_6): δ 9.41 (s, 1H), 8.44 (s, 1H), 7.67 (d, $J = 1.8$ Hz, 1H), 7.66 (s, 1H), 7.47 (d, $J = 7.8$ Hz, 1H), 7.40 (t, $J = 7.8$ Hz, 1H), 7.38 – 7.31 (m, 3H), 7.27 (dd, $J = 9.2$, 4.6 Hz, 2H), 4.92 (d, $J = 13.2$ Hz, 2H), 3.15 (t, $J = 12.0$ Hz, 2H), 2.92 (dd, $J = 13.8$, 10.4 Hz, 1H), 1.88 (d, $J = 11.4$ Hz, 2H), 1.67 (qd, $J = 12.8$, 3.8 Hz, 2H); ^{13}C NMR (100 MHz, DMSO-d_6): δ 181.43, 152.26, 150.88, 148.43, 142.48, 133.61, 130.78, 129.26, 127.68, 127.27, 126.73, 126.00, 125.86, 122.41, 121.12, 120.35, 49.12, 41.79, 32.98. HRMS Calcd. for $C_{21}H_{20}ClN_3OS$ $[M + H]^+$ 398.1089, found 398.1093.

Methyl 2-(1-((3-(oxazol-5-yl)phenyl)carbamothioyl)piperidin-4-yl)acetate (5c)Methyl 2-(1-((3-(oxazol-5-yl)phenyl) carbamothioyl)piperidin-4-yl)acetate (5c) White solid, yield: 50%; mp: 87.5–88.9 ℃; IR (KBr, cm^{-1}):2926, 1730, 1634, 1529, 1442, 1321,1250, 910, 828, 755; ^{1}H NMR (400 MHz, DMSO-d_6): δ 9.33 (s, 1H), 8.44 (s, 1H), 7.64 (d, $J = 5.6$ Hz, 2H), 7.46 (d, $J = 7.8$ Hz, 1H), 7.38 (t, $J = 7.8$ Hz, 1H), 7.29 (d, $J = 8.2$ Hz, 1H), 4.72 (d, $J = 13.2$ Hz, 2H), 3.61 (s, 3H), 3.10 (t, $J = 11.8$ Hz, 2H), 2.32 (d, $J = 7.0$ Hz, 2H), 2.02 (ddd, $J = 16.6$, 8.4, 4.6 Hz, 1H), 1.73 (d, $J = 11.0$ Hz, 2H), 1.30–1.17 (m, 2H); ^{13}C NMR (100 MHz, DMSO-d_6): δ 181.14, 172.76, 152.22, 150.88, 142.46, 129.23, 127.64, 125.84, 122.36, 121.12, 120.31, 51.70, 48.61, 40.14, 32.87, 31.71. HRMS Calcd. for $C_{18}H_{21}N_3O_3S$ $[M + H]^+$ 360.1377, found 360.1379.

4-(4-fluorophenyl)-*N*-(1-methyl-3-phenyl-1*H*-pyrazol-5-yl) piperidine-1-carboth-ioamide (5d) White solid, yield: 61%; mp: 178.2–179.8 ℃; IR (KBr, cm^{-1}): 2931, 1606, 1564, 1509, 1476, 1443, 1363, 1307, 833, 766, 725, 697; ^{1}H NMR (400 MHz, $CDCl_3$): δ 7.80–7.73 (m, 2H), 7.37 (t, $J = 7.6$ Hz, 2H), 7.28 (t, $J = 7.4$ Hz, 1H), 7.17–7.10 (m, 2H), 7.08 (s, 1H), 7.04–6.95 (m, 2H), 6.39 (s, 1H), 4.78 (d, $J = 12.8$ Hz,2H), 3.78 (s, 3H), 3.15 (td, $J = 13.2$,2.4 Hz, 2H), 2.78 (tt, $J = 11.8$, 3.6 Hz, 1H), 1.92 (d, $J = 12.4$ Hz, 2H), 1.73 (ddd, $J = 25.8$, 12.8, 3.8 Hz, 2H);^{13}C NMR (100 MHz, $CDCl_3$): δ 182.18, 161.62 (d, $J = 245.0$ Hz), 149.79, 140.04 (m), 138.86, 133.34, 128.62, 128.09 (d, $J = 7.8$ Hz), 127.76, 125.28, 115.46 (d, $J = 21.2$ Hz), 99.35, 49.71, 41.54, 36.03, 32.99. HRMS Calcd. for $C_{22}H_{23}FN_4S$ $[M + H]^+$ 395.1700, found 395.1707.

4-(3-chlorophenyl)-*N*-(1-methyl-3-phenyl-1*H*-pyrazol-5-yl) piperidine-1-carbo-thioamide (5e) White solid, yield: 55%; mp: 141.2–142.9 ℃; IR (KBr, cm^{-1}): 3198, 3063, 2932, 2856, 1566, 1591, 1498, 1476, 1439, 1319, 1301, 879, 831, 771, 724, 699; ^{1}H NMR (400 MHz, $CDCl_3$): δ 7.77–7.69 (m, 2H), 7.36 (t, $J = 7.6$ Hz, 2H), 7.28 (t, $J = 4.8$ Hz, 1H), 7.25–7.18 (m, 2H), 7.14 (s, 1H), 7.05–6.99 (m, 1H), 6.36 (s, 1H), 4.73 (d, $J = 12.8$ Hz, 2H), 3.72 (s, 3H), 3.15–2.95 (m, 2H), 2.72 (tt, $J = 12.0$, 3.6 Hz, 1H), 1.88 (d, $J = 12.0$ Hz, 2H), 1.67 (qd, $J = 13.0$, 3.8 Hz, 2H); ^{13}C NMR (100 MHz, $CDCl_3$): δ 181.88, 149.65, 146.42, 139.08, 134.43, 133.30, 129.96, 128.70, 127.84, 126.99, 126.89, 125.25, 124.94, 99.62, 49.47, 41.88, 36.03, 32.60. HRMS Calcd. for $C_{22}H_{23}ClN_4S$ $[M + H]^+$ 411.1405, found 411.1408.

Methyl 2-(1-((1-methyl-3-phenyl-1*H*-pyrazol-5-yl)carbamothioyl)piperidin-4-yl)acetate (5f) Yellow solid, yield: 45%; mp: 85.3–86.7 ℃; IR (KBr, cm^{-1}): 2931, 1734, 1628, 1568, 1524, 1442, 1364, 1311, 766, 726, 697, 670; ^{1}H NMR (400 MHz, $CDCl_3$): δ 7.76–7.66 (m, 2H), 7.36 (t, $J = 7.6$ Hz, 2H), 7.31 (s, 1H), 7.30–7.24 (m, 1H), 6.31 (s, 1H), 4.55 (d, $J = 12.4$ Hz, 2H), 3.67 (s, 3H), 3.66 (s, 3H), 3.06–2.88 (m, 2H), 2.23–2.16 (m, 2H), 2.03–1.95 (m, 1H), 1.73 (d, $J = 12.8$ Hz, 2H), 1.25–1.15 (m, 2H); ^{13}C NMR (100 MHz, $CDCl_3$): δ 181.58, 172.58, 149.54, 139.13, 133.33, 128.64, 127.75, 125.23, 99.63, 51.64, 48.98, 40.16, 35.95, 32.51, 31.38. HRMS Calcd. for $C_{19}H_{24}N_4O_2S$ $[M + H]^+$ 373.1693, found 373.1701.

***N*-(3-chloro-4-fluorophenyl)-4-(4-(trifluoromethyl)benzyl) piperazine-1-carbo-thioamide (6a)** White solid, yield: 71%; mp: 164.1–165.3 ℃; IR (KBr, cm^{-1}):3246, 3038, 2925, 2888, 2806, 1620, 1532, 1503, 1458, 1425, 1319, 881, 845, 729; ^{1}H NMR (400 MHz, $CDCl_3$): δ 7.59 (d, $J = 8.0$ Hz, 2H), 7.46 (d, $J = 7.8$ Hz, 2H), 7.24 (s, 1H), 7.16–7.00 (m, 3H), 3.88 (s, 4H), 3.61 (s, 2H), 2.54 (s, 4H); ^{13}C NMR (100 MHz, DMSO-d_6): δ 181.67, 154.61 (d, $J = 243.9$ Hz), 143.35, 138.75 (d, $J = 3.2$ Hz), 129.96, 128.22 (q, $J = 31.7$ Hz), 127.65, 126.33 (d, $J = 7.1$ Hz), 125.58 (q, $J = 3.7$ Hz), 124.83 (q, $J = 271.9$ Hz), 118.72 (d, $J = 18.6$ Hz), 116.42 (d, $J = 21.8$ Hz), 61.30, 52.66, 48.48. HRMS Calcd. for $C_{19}H_{18}ClF_4N_3S$ $[M + H]^+$ 432.0919, found 432.0920.

***N*-(thiazol-2-yl)-4-(4-(trifluoromethyl)benzyl)piperazine-1-carbothioamide (6b)** Yellow solid, yield: 66%; mp: 200.1–201.4 °C; IR (KBr, cm^{-1}):3126, 3030, 2980, 2936, 2857, 2802, 1620, 1526, 1475, 1457, 1365, 788, 756, 695; ^{1}H NMR (400 MHz, DMSO-d_6): δ 12.47 (s, 1H), 7.70 (d, $J = 8.2$ Hz, 2H), 7.57 (d, $J = 8.0$ Hz, 2H), 7.30 (d, $J = 4.6$ Hz, 1H), 6.72 (d, $J = 4.6$ Hz, 1H), 4.05 (s, 4H), 3.61 (s, 2H), 2.41 (s, 4H); ^{13}C NMR (100 MHz, DMSO-d_6): δ 184.20, 170.46, 143.51, 129.93, 128.17 (q, $J = 31.8$ Hz), 125.56 (q, $J = 3.7$ Hz), 124.83 (q, $J = 271.8$ Hz), 123.69 (br), 108.31,

61.49, 52.99. HRMS Calcd. for $C_{16}H_{17}F_3N_4S_2$ $[M+H]^+$ 387.0920, found 387.0926.

***N*-(4-fluorophenyl)-4-(4-(trifluoromethyl)benzyl)piperazine-1-carbothioamide (6c)** White solid, yield: 65%; mp: 170.2–171.8 ℃; IR (KBr, cm^{-1}):3250, 2919, 2816, 1617, 1529, 1425, 1394, 1327, 833, 724, 687; ^{1}H NMR (400 MHz, DMSO-d_6): δ 9.28 (s, 1H), 7.71 (d, J = 8.2 Hz, 2H), 7.57 (d, J = 8.0 Hz, 2H), 7.27 (dd, J = 9.0, 5.2 Hz, 2H), 7.11 (t, J = 8.8 Hz, 2H), 3.96 – 3.85 (m, 4H), 3.63 (s, 2H), 2.48–2.41 (m, 4H); ^{13}C NMR (100 MHz, DMSO-d_6): δ 181.99, 159.63 (d, J = 241.0 Hz), 143.40, 137.80 (d, J = 2.8 Hz), 129.96, 128.21 (q, J = 31.7 Hz), 128.06 (d, J = 8.3 Hz), 125.58 (q, J = 3.6 Hz), 124.84 (q, J = 271.9 Hz), 115.04 (d, J = 22.4 Hz), 61.33, 52.70, 48.37. HRMS Calcd. for $C_{19}H_{19}F_4N_3S$ $[M+H]^+$ 398.1309, found 398.1312.

***N*-(4-chlorophenyl)-4-(4-(trifluoromethyl)benzyl)piperazine-1-carbothioamide (6d)** Yellow solid, yield: 64%; mp: 168.9–169.4 ℃; IR (KBr, cm^{-1}):3255, 2950, 2907, 2814, 1620, 1589, 1527, 1490, 1424, 1392, 1328, 835, 723, 699, 679; ^{1}H NMR (400 MHz, DMSO-d_6): δ 9.35 (s, 1H), 7.71 (d, J = 8.2 Hz, 2H), 7.57 (d, J = 8.0 Hz, 2H), 7.36 – 7.27 (m, 4H), 3.96–3.84 (m, 4H), 3.63 (s, 2H), 2.49–2.38 (m, 4H); ^{13}C NMR (100 MHz, DMSO-d_6): δ 181.71, 143.38, 140.52, 129.96, 128.63, 128.31, 128.21 (q, J = 31.6 Hz), 127.20, 125.58 (q, J = 3.7 Hz), 124.83 (q, J = 272.0 Hz), 61.31, 52.70, 48.51. HRMS Calcd. for $C_{19}H_{19}ClF_3N_3S$ $[M+H]^+$ 414.1013, found 414.1018.

***N*-(1,3-dimethyl-1*H*-pyrazol-5-yl)-4-(4-(trifluoromethyl)benzyl)piperazine-1-carbothioamide (6e)** Yellow solid, yield: 56%; mp: 101.2–102.1 ℃; IR (KBr, cm^{-1}): 3223, 2926, 2816, 1621, 1571, 1491, 1442, 1418, 1370, 1326, 850, 820, 793, 729; ^{1}H NMR (400 MHz, $CDCl_3$): δ 7.59 (d, J = 8.0 Hz, 2H), 7.45 (d, J = 8.0 Hz, 2H), 5.81 (s, 1H), 3.99 – 3.83 (m, 4H), 3.59 (s, 2H), 3.56 (s, 3H), 2.52 (d,J = 4.2 Hz, 4H), 2.18 (s, 3H); ^{13}C NMR (100 MHz, $CDCl_3$): δ 182.38, 146.85, 141.78, 138.59, 129.59 (q, J = 32.2 Hz), 129.19, 125.34 (q, J = 3.8 Hz), 124.20 (q, J = 272.0 Hz), 101.98, 61.92, 52.42, 48.76, 35.27, 14.04. HRMS Calcd. for $C_{18}H_{22}F_3N_5S$ $[M+H]^+$ 398.1621, found 398.1623.

***N*-(3-chlorophenyl)-4-(4-(trifluoromethyl)benzyl)piperazine-1-carbothioamide (6f)** Yellow solid, yield: 66%; mp: 135.1–136.4 ℃; IR (KBr, cm^{-1}):2920, 1645, 1525, 1457, 1427, 1393, 1319, 844, 727, 673; ^{1}H NMR (400 MHz, DMSO-d_6): δ 9.40 (s, 1H), 7.71 (d, J = 8.0 Hz, 2H), 7.57 (d, J = 8.0 Hz, 2H), 7.41 (t, J = 1.8 Hz, 1H), 7.34–7.23 (m, 2H), 7.14 (dd, J = 7.6, 1.8 Hz, 1H), 3.99–3.84 (m, 4H), 3.63 (s, 2H), 2.49–2.43 (m, 4H); ^{13}C NMR (100 MHz, DMSO-d_6): δ 181.55, 143.36, 143.09, 132.55, 129.97, 128.21 (q, J = 31.7 Hz), 125.58 (q, J = 3.8 Hz) 124.89, 124.83 (q, J = 271.8 Hz), 124.20, 123.71, 61.30, 52.68, 48.59. HRMS Calcd. for $C_{19}H_{19}ClF_3N_3S$ $[M+H]^+$ 414.1013, found 414.1017.

***N*-(3,4-dichlorophenyl)-4-(4-(trifluoromethyl)benzyl)piperazine-1-carbothio-amide (6g)** White solid, yield: 67%; mp: 155.8–156.9 ℃; IR (KBr, cm^{-1}):3242, 2922, 2815, 1621, 1578, 1525, 1471, 1421, 1377, 1327, 873, 826, 722, 675; ^{1}H NMR (400 MHz, DMSO-d_6): δ 9.45 (s, 1H), 7.71 (d, J = 8.2 Hz, 2H), 7.61 (d, J = 2.4 Hz, 1H), 7.57 (d, J = 7.8 Hz, 2H), 7.53 (d, J = 8.8 Hz, 1H), 7.32 (dd, J = 8.8, 2.4 Hz, 1H), 3.91 (s, 4H), 3.63 (s, 2H), 2.48–2.44 (m, 4H); ^{13}C NMR (100 MHz, DMSO-d_6): δ 181.36, 143.33, 141.77, 130.47, 130.16, 129.98, 128.21 (q, J = 31.7 Hz), 126.63, 126.23, 125.60 (q, J = 3.4 Hz), 125.29, 124.82 (q, J = 272.1 Hz), 61.27, 52.65, 48.61. HRMS Calcd. for $C_{19}H_{18}Cl_2F_3N_3S$ $[M+H]^+$ 448.0624, found 448.0627.

***N*-(4,4-dimethylcyclohexyl)-4-(4-(trifluoromethyl)benzyl) piperazine-1-carbothio-amide (6h)** White solid, yield: 72%; mp: 132.1–133.8 ℃; IR (KBr, cm^{-1}):3346, 2942, 2865, 2807, 2764, 1623, 1537, 1454, 1414, 1348, 1323, 883, 838, 800, 704, 673; ^{1}H NMR (400 MHz, DMSO-d_6): δ 7.69 (d, J = 8.0 Hz, 2H), 7.55 (d, J = 8.0 Hz, 2H), 7.25 (d, J = 7.8 Hz, 1H), 4.20–4.07 (m, 1H), 3.82–3.72 (m, 4H), 3.59 (s, 2H), 2.42–2.31 (m, 4H), 1.75–1.60 (m, 2H), 1.46 (td, J = 13.2, 3.2 Hz, 2H), 1.35 (d, J = 12.6 Hz, 2H), 1.19 (td, J = 13.4, 3.4 Hz, 2H), 0.90 (d, J = 8.0 Hz, 6H).; ^{13}C NMR (100 MHz, DMSO-d_6): δ 180.81, 143.43, 129.93, 128.17 (q, J = 31.7 Hz), 125.55 (q, J = 3.8 Hz), 124.83 (q, J = 271.9 Hz), 61.41, 55.09, 52.72, 47.62, 38.39, 32.79, 29.81, 28.08, 24.45. HRMS Calcd. for $C_{21}H_{30}F_3N_3S$ $[M+H]^+$ 414.2186, found 414.2190.

***N*-(4-bromophenyl)-4-(4-(trifluoromethyl)benzyl)piperazine-1-carbothioamide (6i)** White solid, yield: 65%; mp: 160.1–161.9 ℃; IR (KBr, cm^{-1}):3257, 2940, 2804, 1628, 1586, 1525, 1485, 1420, 1324, 819, 712, 672, 649; ^{1}H NMR (400 MHz, DMSO-d_6): δ 9.35 (s, 1H), 7.71 (d, J = 8.2 Hz, 2H), 7.57 (d, J = 8.0 Hz, 2H), 7.50–7.40 (m, 2H), 7.26 (d, J = 8.8 Hz, 2H), 3.96–3.84 (m, 4H), 3.63 (s, 2H), 2.49–2.40 (m, 4H); ^{13}C NMR (100 MHz, DMSO-d_6): δ 181.64, 143.32, 140.95, 131.24, 129.98, 128.21 (q, J = 31.6 Hz), 127.52, 125.57 (q, J = 3.7 Hz), 124.82 (q, J = 272.0 Hz), 116.78, 61.31, 52.68, 48.51. HRMS Calcd. for $C_{19}H_{19}BrF_3N_3S$ $[M+H]^+$ 458.0508, found 458.0521.

***N*-(naphthalen-1-yl)-4-(4-(trifluoromethyl)benzyl)piperazine-1-carbothio-amide (6j)** Pink solid, yield: 61%; mp: 139.9–140.8 ℃; IR (KBr, cm^{-1}): 3250,2907, 2810, 1620, 1598, 1514, 1416, 1392, 1327, 842, 798, 774, 694; ^{1}H NMR (400 MHz, DMSO-d_6): δ 9.48 (s, 1H), 7.95–7.87 (m, 1H), 7.85–7.77 (m, 2H), 7.72 (d, J = 8.2 Hz, 2H), 7.59 (d,

$J = 8.0$ Hz, 2H), 7.53–7.44 (m, 3H), 7.29 (d, $J = 7.2$ Hz, 1H), 4.08–3.93 (m, 4H), 3.66 (s, 2H), 2.52 (d, $J = 4.8$ Hz, 4H); ^{13}C NMR (100 MHz, DMSO-d_6): δ 183.03, 143.43, 137.80, 134.27, 131.14, 130.00, 128.40, 128.22 (q, $J = 32.1$ Hz), 126.89, 126.42, 126.31, 126.27, 125.98, 125.59 (q, $J = 3.8$ Hz), 124.85 (q, $J = 272.0$ Hz), 124.17, 61.39, 52.81, 48.44. HRMS Calcd. for $C_{23}H_{22}F_3N_3S$ $[M + H]^+$ 430.1560, found 430.1570.

4-(4-(trifluoromethyl)benzyl)-*N*-(4-(trifluoromethyl)phenyl) piperazine-1-carbothioamide (6k) Yellow solid, yield: 64%; mp: 131.2–132.6 ℃; IR (KBr, cm^{-1}): 3236, 2953, 2918, 2812, 1618, 1595, 1531, 1479, 1431, 1399, 1323, 843, 741, 703; ^{1}H NMR (400 MHz, DMSO-d_6): δ 9.57 (s, 1H), 7.71 (d, $J = 8.2$ Hz, 2H), 7.63 (d, $J = 8.6$ Hz, 2H), 7.58 (d, $J = 8.0$ Hz, 2H), 7.53 (d, $J = 8.6$ Hz, 2H), 4.00–3.85 (m, 4H), 3.64 (s, 2H), 2.47 (d, $J = 5.0$ Hz, 4H); ^{13}C NMR (100 MHz, DMSO-d_6): δ 181.56, 145.42, 143.35, 129.97, 128.22 (q, $J = 31.6$ Hz), 125.55 (m), 124.93 (q, $J = 271.3$ Hz), 124.83 (q, $J = 272.0$ Hz), 124.51, 124.09 (q, $J = 32.0$ Hz), 61.27, 52.69, 48.76. HRMS Calcd. for $C_{20}H_{19}F_6N_3S$ $[M + H]^+$ 448.1277, found 448.1281.

***N*-([1,1′-biphenyl]-4-yl)-4-(4-(trifluoromethyl)benzyl)piperazine-1-carbothio-amide (6l)** Yellow solid, yield: 66%; mp: 133.2–134.9 ℃; IR (KBr, cm^{-1}): 2929, 1742, 1646, 1539, 1455, 1422, 1330, 838, 763, 727, 693;^{1}H NMR (400 MHz, DMSO-d_6): δ 9.38 (s, 1H), 7.71 (d, $J = 8.2$ Hz, 2H), 7.65 (d, $J = 7.2$ Hz, 2H), 7.59 (dd, $J = 8.2$, 5.0 Hz, 4H), 7.45 (t, $J = 7.8$ Hz, 2H), 7.38 (d, $J = 8.6$ Hz, 2H), 7.34 (t, $J = 7.4$ Hz, 1H), 3.92 (s, 4H), 3.64 (s, 2H), 2.47 (d, $J = 5.0$ Hz, 4H); ^{13}C NMR (100 MHz, DMSO-d_6): δ 181.76, 143.40, 141.00, 140.25, 136.30, 129.97, 129.38, 128.21 (q, $J = 31.6$ Hz), 127.57, 126.83, 126.65, 125.74, 125.59 (q, $J = 3.8$ Hz), 124.84 (q, $J = 271.9$ Hz), 61.34, 52.74, 48.55. HRMS Calcd. for $C_{25}H_{24}F_3N_3S$ $[M + H]^+$ 456.1716, found 456.1718.

***N*-(4-isopropylphenyl)-4-(4-(trifluoromethyl)benzyl)piperazine-1-carbothio-amide (6m)** Yellow solid, yield: 69%; mp: 166.1–168.5 ℃; IR (KBr, cm^{-1}): 2961, 2808, 1621, 1588, 1529, 1462, 1420, 1395, 1325, 843, 741, 703; ^{1}H NMR (400 MHz, DMSO-d_6): δ 9.21 (s, 1H), 7.71 (d, $J = 8.2$ Hz, 2H), 7.57 (d, $J = 8.0$ Hz, 2H), 7.21–7.10 (m, 4H), 3.96–3.83 (m, 4H), 3.63 (s, 2H), 2.85 (dq, $J = 13.8$, 7.0 Hz, 1H), 2.48–2.40 (m, 4H), 1.19 (d, $J = 7.0$ Hz, 6H); ^{13}C NMR (100 MHz, DMSO-d_6): δ 181.86, 144.87, 143.41, 139.17, 129.96, 128.19 (q, $J = 31.6$ Hz), 126.23, 126.19, 125.77, 125.58 (q, $J = 3.4$ Hz), 124.84 (q, $J = 271.9$ Hz), 61.34, 52.73, 48.37, 33.39, 24.43. HRMS Calcd. for $C_{22}H_{26}F_3N_3S$ $[M + H]^+$ 422.1873, found 422.1877.

***N*-(3-(oxazol-5-yl)phenyl)-4-(4-(trifluoromethyl)benzyl)piperazine-1-carbothio-amide (6n)** White solid, yield: 67%; mp: 137.2–139.1 ℃; IR (KBr, cm^{-1}): 2918, 2810, 1619, 1593, 1532, 1467, 1426, 1325, 847, 822, 791, 723, 687; ^{1}H NMR (400 MHz, DMSO-d_6): δ 9.43 (s, 1H), 8.44 (s, 1H), 7.72 (d, $J = 8.2$ Hz, 2H), 7.66 (s, 2H), 7.58 (d, $J = 8.0$ Hz, 2H), 7.47 (d, $J = 7.8$ Hz, 1H), 7.40 (t, $J = 7.8$ Hz, 1H), 7.31 (d, $J = 8.2$ Hz, 1H), 3.93 (m, 4H), 3.65 (s, 2H), 2.52–2.48 (m, 4H); ^{13}C NMR (100 MHz, $CDCl_3$): δ 183.13, 150.87, 150.63, 141.75, 140.71, 129.75, 129.70 (q, $J = 32.3$ Hz), 129.17, 128.65, 125.35 (q, $J = 3.8$ Hz), 124.15 (q, $J = 272.0$ Hz), 123.13, 122.08, 121.00, 118.81, 62.02, 52.39, 49.42. HRMS Calcd. for $C_{22}H_{21}F_3N_4OS[M + H]^+$ 447.1461, found 447.1460.White solid, yield: 67%; mp: 137.2–139.1 ℃; IR (KBr, cm^{-1}): 2918, 2810, 1619, 1593, 1532, 1467, 1426, 1325, 847, 822, 791, 723, 687; ^{1}H NMR (400 MHz, DMSO-d_6): δ 9.43 (s, 1H), 8.44 (s, 1H), 7.72 (d, $J = 8.2$ Hz, 2H), 7.66 (s, 2H), 7.58 (d, $J = 8.0$ Hz, 2H), 7.47 (d, $J = 7.8$ Hz, 1H), 7.40 (t, $J = 7.8$ Hz, 1H), 7.31 (d, $J = 8.2$ Hz, 1H), 3.93 (m, 4H), 3.65 (s, 2H), 2.52–2.48 (m, 4H); ^{13}C NMR (100 MHz, $CDCl_3$): δ 183.13, 150.87, 150.63, 141.75, 140.71, 129.75, 129.70 (q, $J = 32.3$ Hz), 129.17, 128.65, 125.35 (q, $J = 3.8$ Hz), 124.15 (q, $J = 272.0$ Hz), 123.13, 122.08, 121.00, 118.81, 62.02, 52.39, 49.42. HRMS Calcd. for $C_{22}H_{21}F_3N_4OS[M + H]^+$ 447.1461, found 447.1460.

***N*-(1-methyl-3-phenyl-1*H*-pyrazol-5-yl)-4-(4-(trifluoromethyl) benzyl)piperazine-1-carbothioamide (6o)** Light yellow solid, yield: 62%; mp: 187.4–188.1 °C; IR (KBr, cm^{-1}): 3217, 3020, 2924, 2821, 1622, 1559, 1528, 1447, 1327, 855, 819, 763, 699; ^{1}H NMR (400 MHz, DMSO-d_6): δ 9.31 (s, 1H), 7.76 (d, $J = 7.2$ Hz, 2H), 7.72 (d, $J = 8.2$ Hz, 2H), 7.58 (d, $J = 8.0$ Hz, 2H), 7.38 (t, $J = 7.6$ Hz, 2H), 7.27 (t, $J = 7.4$ Hz, 1H), 6.52 (s, 1H), 3.95 (s, 4H), 3.65 (s, 2H), 3.62 (s, 3H), 2.47 (d, $J = 4.8$ Hz, 4H); ^{13}C NMR (100 MHz, DMSO-d_6): δ 181.83, 148.20, 143.35, 140.40, 134.04, 129.98, 129.05, 128.23 (q, $J = 31.7$ Hz), 127.74, 125.60 (q, $J = 3.8$ Hz), 125.08, 124.84 (q, $J = 272.0$ Hz), 100.33, 61.26, 52.63, 48.62, 36.08. HRMS Calcd. for $C_{23}H_{24}F_3N_5S$ $[M + H]^+$ 460.1778, found 460.1782.

Biological assays

General

A2780 (human ovarian cancer cell lines), MDA-MB-468, MDA-MB-231 (human breast cancer cell lines) and HEK293T (human embryonic kidney cell lines) were purchased from American Type Culture Collection (ATCC). Cells were maintained in RPMI-1640 media or DMEM media (Gibco) supplemented with 10% fetal bovine serum (Hyclone), 100 U ml^{-1} penicillin (Sigma-Aldrich, USA) and 100 μg ml^{-1} streptomycin (Sigma-Aldrich, USA) at 37 ℃ in a humidified atmosphere containing 5% CO_2. All tumor cell

lines were maintained according to the ATCC procedures. All enzyme assay reagents were purchased from Ronghai Huakang Biotechnology.

Enzyme assays

The inhibitory activity of all the synthesized compounds (**4a**–**b**, **5a**–**f**, **6a**–**o**) against PHGDH was evaluated. The experimental schematic is illustrated in Fig. 2 (Wang et al. 2017). Briefly, 1 µl of test compounds and 50 µl of PHGDH (final concentration was 200 nM) were added to the opaque 96-well plate, followed by incubation for 1 h. Then, 49 µl of mixtures (0.1 mM resazurin; 0.001 U/µl diaphorase; 1 mM hydrazine sulfate; 20 µM NAD^+; 0.1 mM 3-PG; the above were the final concentration) was added to each well. 3-PG is not in the blank control group. Mixtures were further incubated for 1 h. The resulting fluorescence was read using a ViewLux uHTS Microplate Imager (PerkinElmer). PHGDH inhibition data were calculated by using the following formula: inhibition rate $= 1 - (F_{compound} - F_{No\text{-}3PG})/(F_{DMSO} - F_{No\text{-}3PG})$. $F_{compound}$ was resorufin fluorescence of compound well; F_{DMSO} was resorufin fluorescence of DMSO well; and $F_{No\text{-}3PG}$ was resorufin fluorescence of nonsubstrate well. IC_{50} values were calculated by Graph-Pad Prism 7 software (San Diego, USA) using XY modeling. **NCT-503** was used as positive control.

To exclude false positive molecules which inhibited diaphorase, exclusion experiments were performed on the active molecules screened. One microliter (1 mM) of test compounds, positive control (DMSO) and negative control (no NADH) was added to the opaque 96-well plates, respectively. Then, 50 µl of diaphorase (0.001 U/µl, the final concentration) was added followed by incubation for 1 h. After that, 49 µl of mixtures (0.1 mM resazurin; 10 µM NADH) was added to each well and incubated for 30 min. The data were analyzed as described above.

MTT assay

The anti-proliferative activity of selected PHGDH- active compounds (**4a**, **5a**, **6e**, **6n** and **NCT-503**) against cancer cell lines was evaluated by MTT assay. Briefly, cell lines were seeded in 96-well plate at 2000 cells per well and then treated with compounds for 72 h. Ten microliters of MTT (10 mg/ml) was added and incubated for another 2.5 h at 37 °C. Then, the supernatant fluid was removed and 150 µl/well DMSO was added for 15–20 min. The absorbance (OD) of each well was measured at 450 nm by SpectraMAX M5 microplate spectrophotometer (Molecular Devices, CA, USA). The inhibition rates were calculated and IC_{50} values were calculated by Graph-Pad Prism 7 software (San Diego, USA) using XY modeling (Nguyen et al. 2018).

Molecular docking and 2D simulation

The molecular docking procedure was performed by using glide docking program of Maestro. A crystal structure of the catalytic subunit of PHGDH (amino acids (aa) 3-314) with cofactor, NAD^+, and substrate analogue, L-malate (1), has been reported (PDB: 2G76) (Kujundzic et al. 2019). The active site was close to NAD^+ in this structure (Kujundzic et al. 2019). Therefore, the crystal structure of 2G76 was selected to perform molecular docking. Briefly, the structure 2G76 was downloaded and optimized into receptor protein. Then, receptor grid was generated. The square area centered on NAD^+ was set as the docking pocket; 200,000 small molecule database was then used to dock using standard precision. Finally, 2D interaction diagrams of docking molecules were simulated based on the data of docking.

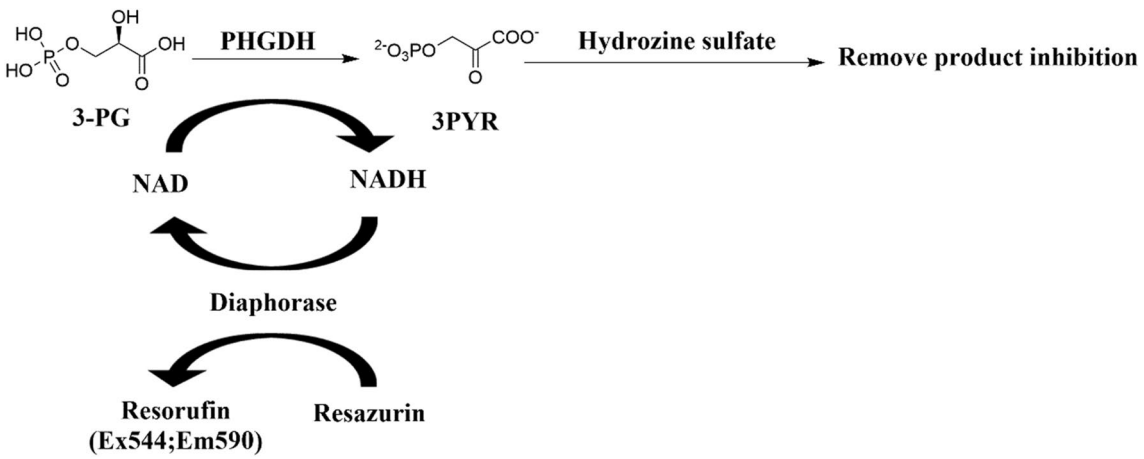

Fig. 2 Experimental schematic of PHGDH activity assay in vitro

Results and discussion

Chemistry

The synthetic routes of compounds **4a**–**b**, **5a**–**f** and **6a**–**o** are depicted in Scheme 1. Structures of all synthesized compounds are shown in Tables 1 and 2. Compound **116** was obtained by one-step reaction, amide condensation (Zhang et al. 2018). The synthesis of compounds **4a**–**b**, **5a**–**f** and **6a**–**o** involved the formation of thiourea bonds (Hemdan and El-Bordany 2016). One-pot method was applied in this synthesis process. Firstly, aromatic amine and TCDI formed active intermediate. The intermediate was then reacted with the piperazine or piperidine derivative added later to form the expected product. The average yield of entire reaction process was 62%.

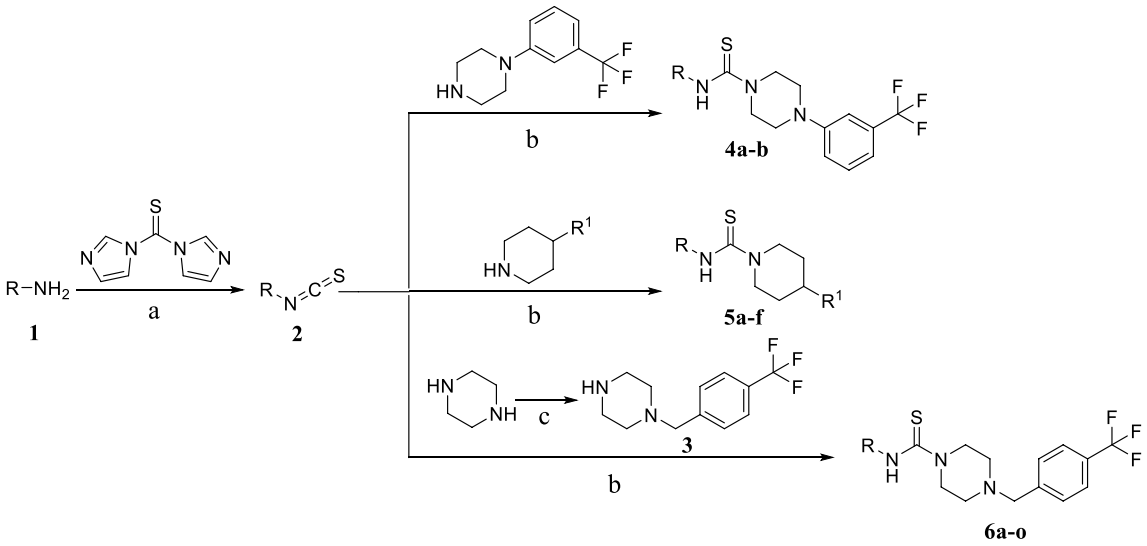

Scheme 1 Conditions: **a** di(1*H*-imidazol-1-yl)methanethione, THF, 45 °C, 0.5–1.5 h; **b** piperazine or piperidine derivatives, Et_3N, THF, heat to 75 °C, 1.5–2.5 h, 45–72%; **c** 1-(bromomethyl)-4-(trifluoromethyl)benzene, THF, reflux, overnight, 86%

Table 1 Structure of compounds **5a**–**f**

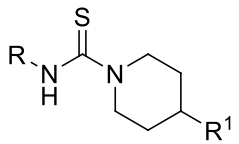

5a-f

Comp	R	R^1	Comp	R	R^1
5a	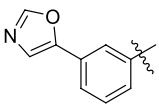	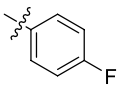	**5b**	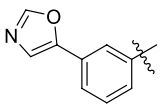	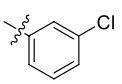
5c	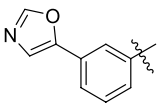	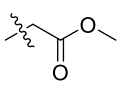	**5d**	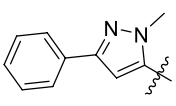	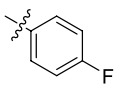
5e	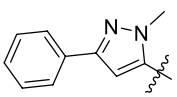	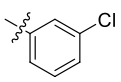	**5f**	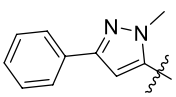	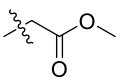

Table 2 Structure of compounds **4a–b** and **6a–o**

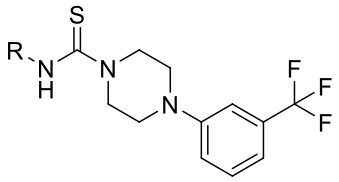

4a-b

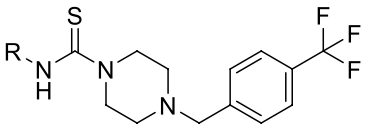

6a-o

Comp	R	Comp	R
4a	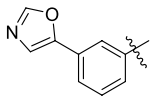	**4b**	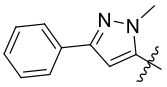
6a	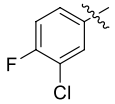	**6b**	
6c	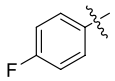	**6d**	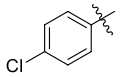
6e	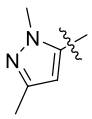	**6f**	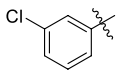
6g	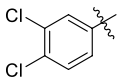	**6h**	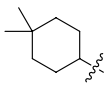
6i	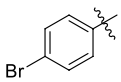	**6j**	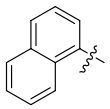
6k	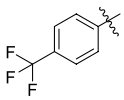	**6l**	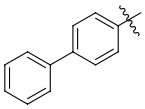
6m	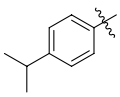	**6n**	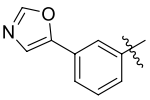
6o	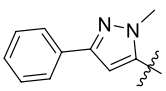		

Biology

Enzyme assays

The inhibitory activity of synthesized compounds against PHGDH was evaluated. The results are shown in Table 3.

Structure–activity relationship analysis It can be seen from Table 3 that the IC_{50} value of **NCT-503** measured by our enzyme activity system was 16 μM. It differs from previously reported data by less than an order of magnitude. Therefore, we thought it was reasonable. Compound **5d** from virtual screening displayed better inhibitory activity against PHGDH than **116**; Furthermore, six other derivatives **4a**, **5a–b**, **6e**, **6n–o** from **5d** showed better activity at 25 μM. However, the other compounds showed low or no activity against PHGDH. Among the six derivatives of better activity, **4a** showed the best inhibitory activity toward

Table 3 Inhibitory activity of compounds against PHGDH in vitro

Compound No.	Structure	Inh%		IC_{50} (μM)
		10 μM	25 μM	
5d	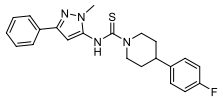	26	30	56
5e	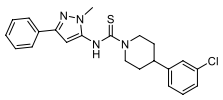	10	23	ND
5f	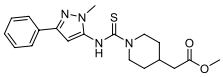	9	24	ND
4b	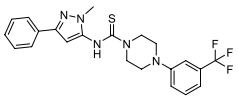	19	20	ND
6o	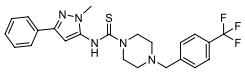	10	31	60
6a	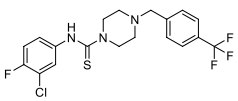	7	16	ND
6b	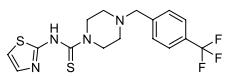	14	30	54
6c	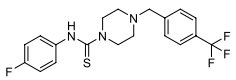	8	15	ND
6d	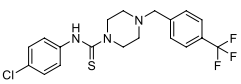	8	16	ND
6e	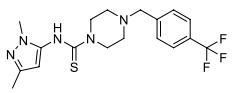	15	38	36
6f	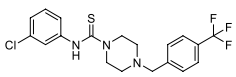	19	25	ND
6g	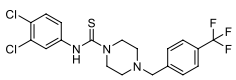	13	20	ND
6h	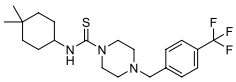	15	17	ND
6i	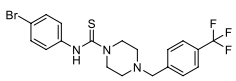	14	22	ND

Table 3 (continued)

Compound No.	Structure	Inh%		IC_{50} (μM)
		10 μM	25 μM	
6j	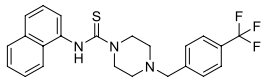	9	9	ND
6k	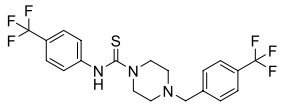	9	12	ND
6l	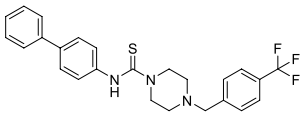	12	26	ND
6m	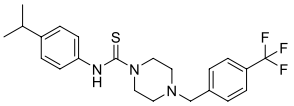	8	14	ND
6n	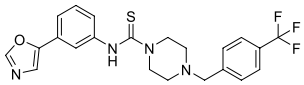	21	47	27
4a	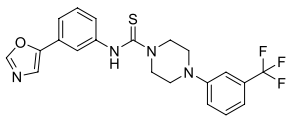	8	65	18
5a	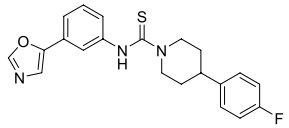	30	49	25
5b	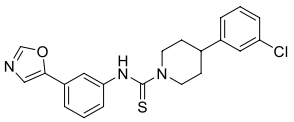	18	32	51
5c	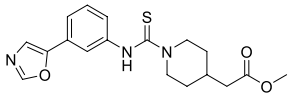	8	24	ND
NCT-503	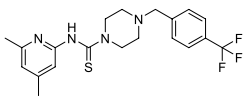	43	67	16
116	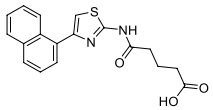	ND	ND	174

[a]Inh% values represent the inhibition rates of compounds at 10 μM or 25 μM. Values are the mean of three repeated experiments. *ND* not detected

Table 4 IC_{50} values of compounds against human cancer cell lines in vitro

Compound no.	IC_{50} (μM)			
	A2780	MDA-MB-468	MDA-MB-231	HEK293T
4a	15.58	9.91	63.42	40.53
5a	7.73	13.05	107.1	55.22
6e	27.86	31.06	123.4	34.63
6n	4.74	7.52	30.13	17.34
NCT-503	22.18	33.95	> 160	60.24

PHGDH with IC_{50} value 18 μM, while **5a** and **6n** had the similar inhibition activity with IC_{50} about 25 μM. In addition, compounds **5b**, **6b**, **6e** displayed IC_{50} which was lower than 55 μM. The preliminary SAR showed that R group of heterocycle was crucial for maintaining PHGDH activity, while those with R group of phenyl, naphthyl or alkyl displayed low inhibitory activity. Generally, compounds with 3-(oxazol-5-yl) phenyl displayed better activity than compounds with other R group, such as **4a**, **5a**–**b** and **6n**. Among the compounds containing different piperazine or piperidine structures, those with fluorine substituents at the end commonly had better PHGDH inhibitory activity. Finally, compounds with low IC_{50} were screened to perform cell proliferation inhibition experiment.

Anti-proliferative activity against human cancer cells lines in vitro Knockdown of PHGDH is selectively toxic toward PHGDH-dependent cell lines and minimally toxic toward PHGDH-independent cell lines. Therefore, treatment of PHGDH-independent cell lines and PHGDH-dependent cell lines in dose–response assays with PHGDH inhibitors could demonstrate that PHGDH inhibitors had a good inhibitory activity against PHGDH (Pacold et al. 2016).

MDA-MB-468 and A2780 were PHGDH high-expression cell lines and PHGDH-dependent. However, MDA-MB-231 was PHGDH low-expression cell lines and PHGDH-independent. We could judge whether a compound acted on PHGDH by activity difference toward cell lines (MDA-MB-468, A2780, MDA-MB-231). Human embryonic kidney cell line HEK293T was used to assess the toxicity to normal human cell. We further evaluated the anti-proliferative activity of compounds **4a**, **5a**, **6e** and **6n**, which could inhibit the PHGDH activity. The results are shown in Table 4.

From Table 4, we can see that **6n**, which contains 3-(oxazol-5-yl) phenyl, was the most active compound in the MTT assay, with an IC_{50} value of 4.74 μM against A2780 and an IC_{50} value of 7.52 μM against MDA-MB-468. It indicated **6n** had a good cellular potency against PHGDH high-expression cell lines. In addition, these compounds had relatively higher IC_{50} values against PHGDH low-expression cell line MDA-MB-231 and human embryonic kidney cell line HEK293T. This indicated that they had good selectivity and low toxicity.

Interaction prediction We docked the active molecules **4a**, **5a**, **6e** and **6n**, predicted and analyzed the 2D diagram of their interactions with the surrounding amino acid residues (Fig. 3). In summary, oxazole formed *pi–pi* conjugation with residues close to it. This moiety was indispensable for maintaining the interactions, which was consistent with structure–activity analysis above. In addition, hydrogen on the thiourea formed hydrogen bond with surrounding residues. Other moieties such as thiocarbonyl and substituted piperazine were essential to keep the suitable configuration that made the molecule go into the groove.

Conclusions

We have designed and synthesized a novel series of thiourea derivatives, according to the structural characteristics of PHGDH inhibitor **5d**. These newly synthesized compounds were characterized by IR, MS, ^{1}H NMR and ^{13}C NMR. Six other derivatives from **5d** showed better activity toward PHGDH. Compound **4a** displayed the best inhibitory activity on PHGDH with IC_{50} of 18 μM. The anti-proliferative activity of four compounds against four cell lines (A2780, MDA-MB-468, MDA-MB-231 and 293 T) was evaluated by MTT assay, and compounds with good anti-proliferative activity and low toxicity were discovered. Finally, 2D interaction diagrams revealed potential action modes of active compounds with PHGDH. From the previous discussion of SAR, we obtained that the enzyme activity of compound was better when the R group was 3-(oxazol-5-yl) phenyl, 1-methyl-3-phenyl-1*h*-pyrazol-5-yl or 1, 3-dimethyl-1*h*-pyrazol-5-yl. In addition, we found that heterocyclic groups played a key role in the interaction between molecules and proteins. Based on the information above, we concluded that compounds were more likely to be active when the R group was heterocyclic. Therefore, this research provided supporting information for further design and synthesis of PHGDH inhibitors.

Acknowledgements We thank State Key Laboratory of Biotherapy, West China Hospital, Sichuan University for ^{1}H NMR, ^{13}C NMR and HRMS determination. We thank Engineering Teaching Experiment Center, School of Chemical Engineering for IR determination. This work was supported by National S&T Major project (2018ZX09201018), Project of the National Keypoint Research and

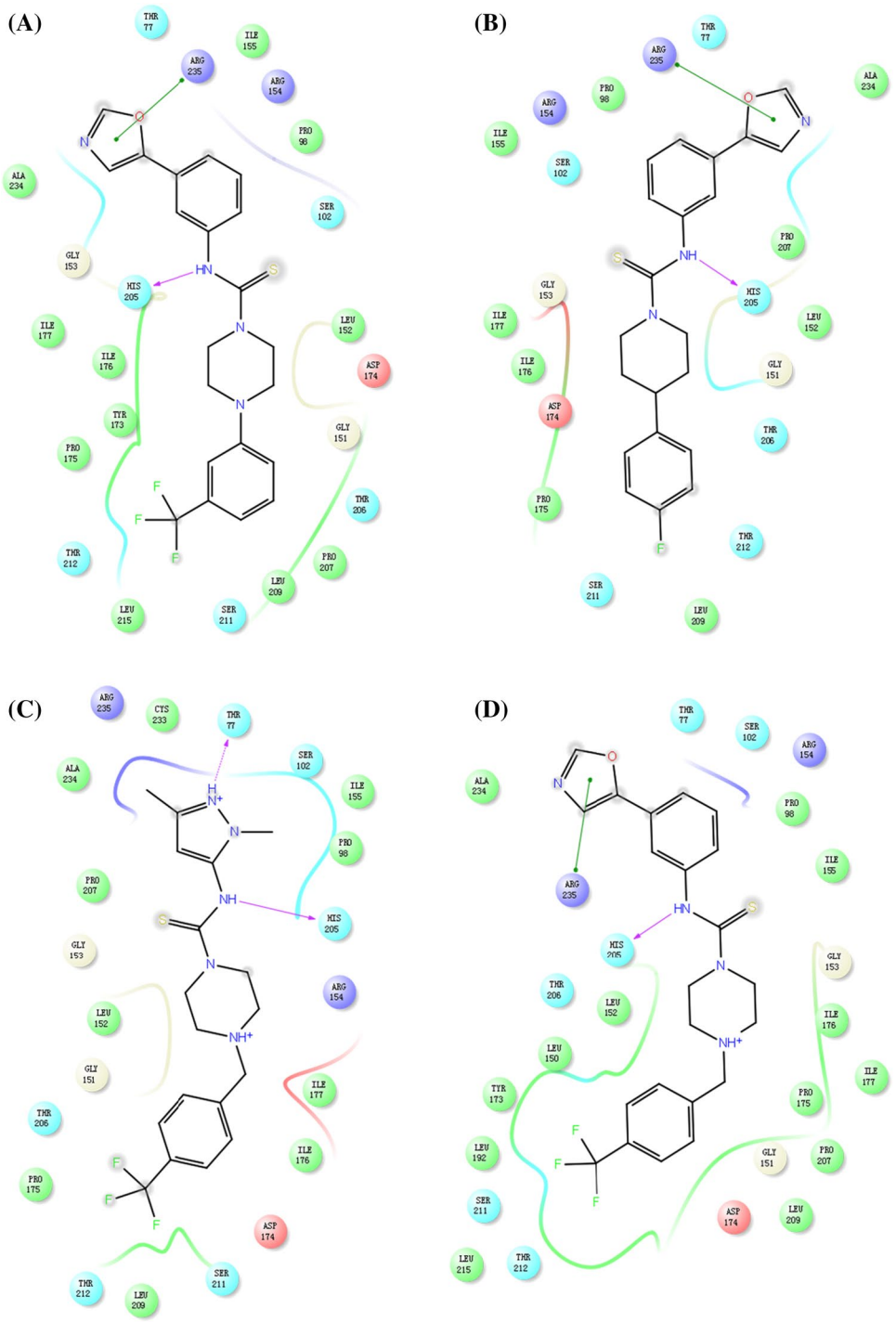

Fig. 3 2D interaction diagrams of **4a**, **5a**, **6e**, **6n**. **a–d** were interaction simulations of **4a**, **5a**, **6e**, **6n** with surrounding amino acid residues, respectively. Arrows represent hydrogen bonds, and round headlines represent *pi–pi* conjugation

Invention Program of China Ministry of Science and Technology (MOST-2016YFC1303200) and National Natural Science Foundation of China (81773198).

Compliance with ethical standards

Conflict of interest On behalf of all authors, the corresponding author states that there is no conflict of interest.

References

Ducker GS, Ghergurovich JM, Mainolfi N et al (2017) Human SHMT inhibitors reveal defective glycine import as a targetable metabolic vulnerability of diffuse large B-cell lymphoma. Proc Natl Acad Sci USA 114:11404–11409. https://doi.org/10.1073/pnas.1706617114

Gromova I, Gromov P, Honma N et al (2015) High level PHGDH expression in breast is predominantly associated with keratin 5-positive cell lineage independently of malignancy. Mol Oncol 9:1636–1654. https://doi.org/10.1016/j.molonc.2015.05.003

Hemdan MM, El-Bordany EA (2016) Use of dodecanoyl isothiocyanate as building block in synthesis of target benzothiazine, quinazoline, benzothiazole and thiourea derivatives. Chem Pap 70:1117–1125. https://doi.org/10.1515/chempap-2016-0042

Jia XQ, Zhang S, Zhu HJ et al (2016) Increased expression of PHGDH and prognostic significance in colorectal cancer. Transl Oncol 9:191–196. https://doi.org/10.1016/j.tranon.2016.03.006

Jing Z, Heng W, Xia L et al (2015) Downregulation of phosphoglycerate dehydrogenase inhibits proliferation and enhances cisplatin sensitivity in cervical adenocarcinoma cells by regulating Bcl-2 and caspase-3. Cancer Biol Ther 16:541–548. https://doi.org/10.1080/15384047.2015.1017690

Kujundzic RN, Stepanic V, Milkovic L et al (2019) Curcumin and its potential for systemic targeting of inflamm-aging and metabolic reprogramming in cancer. Int J Mol Sci 20:1180. https://doi.org/10.3390/ijms20051180

Mattaini KR, Brignole EJ, Kini M et al (2015) An epitope tag alters phosphoglycerate dehydrogenase structure and impairs ability to support cell proliferation. Cancer Metab 3:5. https://doi.org/10.1186/s40170-015-0131-7

Mullarky E, Xu J, Robin AD et al (2019) Inhibition of 3-phosphoglycerate dehydrogenase (PHGDH) by indole amides abrogates de novo serine synthesis in cancer cells. Bioorg Med Chem Lett 29:2503–2510. https://doi.org/10.1016/j.bmcl.2019.07.011

Nguyen DT, Truong GN, Van Vuong T et al (2018) Synthesis of new indirubin derivatives and their in vitro anticancer activity. Chem Pap 73:1083–1092. https://doi.org/10.1007/s11696-018-0659-4

O'Dowd B, Williams S, Wang H et al (2017) Spectroscopic and computational investigations of ligand binding to IspH: discovery of non-diphosphate inhibitors. ChemBioChem 18:914–920. https://doi.org/10.1002/cbic.201700052

Ou Y, Wang SJ, Jiang L et al (2015) p53 Protein-mediated regulation of phosphoglycerate dehydrogenase (PHGDH) is crucial for the apoptotic response upon serine starvation. J Biol Chem 290:457–466. https://doi.org/10.1074/jbc.M114.616359

Pacold ME, Brimacombe KR, Chan SH et al (2016) A PHGDH inhibitor reveals coordination of serine synthesis and one-carbon unit fate. Nat Chem Biol 12:452–458. https://doi.org/10.1038/nchembio.2070

Ravez S, Corbet C, Spillier Q (2017) Alpha-ketothioamide derivatives: a promising tool to interrogate phosphoglycerate dehydrogenase (PHGDH). J Med Chem 60:1591–1597. https://doi.org/10.1021/acs.jmedchem.6b01166

Reid MA, Allen AE, Liu S et al (2018) Serine synthesis through PHGDH coordinates nucleotide levels by maintaining central carbon metabolism. Nat Commun 9:5442. https://doi.org/10.1038/s41467-018-07868-6

Rohde JM, Brimacombe KR, Liu L et al (2018) Discovery and optimization of piperazine-1-thiourea-based human phosphoglycerate dehydrogenase inhibitors. Bioorgan Med Chem 26:1727–1739. https://doi.org/10.1016/j.bmc.2018.02.016

Sullivan MR, Mattaini KR, Dennstedt EA et al (2019) Increased serine synthesis provides an advantage for tumors arising in tissues where serine levels are limiting. Cell Metab 29(1410–1421):e1414. https://doi.org/10.1016/j.cmet.2019.02.015

Truong V, Huang S, Dennis J et al (2017) Blood triglyceride levels are associated with DNA methylation at the serine metabolism gene PHGDH. Sci Rep-UK. https://doi.org/10.1038/s41598-017-09552-z

Vandekeere S, Dubois C, Kalucka J et al (2018) Serine synthesis via PHGDH is essential for heme production in endothelial cells. Cell Metab 28(573–587):e513. https://doi.org/10.1016/j.cmet.2018.06.009

Wang Q, Liberti MV, Liu P et al (2017) Rational design of selective allosteric inhibitors of PHGDH and serine synthesis with antitumor activity. Cell chem biol 24:55–65. https://doi.org/10.1016/j.chembiol.2016.11.013https://doi.

Weinstabl H, Treu M, Rinnenthal J et al (2019) Intracellular trapping of the selective phosphoglycerate dehydrogenase (PHGDH) inhibitor BI-4924 disrupts serine biosynthesis. J Med Chem 62:7976–7997. https://doi.org/10.1021/acs.jmedchem.9b00718

Won S, Park YS, Yoo J et al (2003) Rational design of an indolebutanoic acid derivative as a novel aldose reductase inhibitor based on docking and 3D QSAR studies of phenethylamine derivatives. J Med Chem 46:5619–5627. https://doi.org/10.1021/jm0205346

Zhang Z-H, Wu HM, Deng SN et al (2018) Synthesis and biological evaluation of 2,4-disubstituted thiazole amide derivatives as anticancer agent. Chem Pap 73:355–364. https://doi.org/10.1007/s11696-018-0587-3